Nonlinear Processes
in Geophysics

Open Access

EGU

Discussions

Seasonal predictability of the winter precipitation over Iberian Peninsula and its relationship with finite-time Lyapunov exponents

Daniel Garaboa-Paz[1], Nieves Lorenzo[2], and Vicente Pérez-Muñuzuri[1]

[1]Group of Nonlinear Physics. Faculty of Physics. University of Santiago de Compostela. 15782 Santiago de Compostela, Spain.
[2]Ephyslab. Faculty of Sciences, Campus de Ourense, University of Vigo, 32004 Ourense, Spain.

Correspondence to: V. Pérez-Muñuzuri
(vicente.perez@cesga.es)

Abstract. Seasonal forecasts have improved during the last decades, mostly due to an increase of understanding of the coupled ocean-atmosphere dynamics, and the development of models able to predict the atmosphere variability. Correlations between different teleconnection patterns and severe weather in different parts of the world have also evolved during the last years. This paper evaluates the connection between winter precipitation over the Iberian Peninsula and the large-scale tropospheric mixing over the eastern Atlantic ocean. Finite-time Lyapunov exponents (FTLE) have been calculated from 1979 to 2008 to evaluate this mixing. Our study suggests that significant negative correlations exist between summer FTLE anomalies and winter precipitation over Portugal and Spain. To understand the mechanisms behind this correlation, summer anomalies of the FTLE have also been correlated to other circulation and temperature patterns as the sea surface temperature (SST), the sea level pressure (SLP) or the geopotential. The East Atlantic (EA) teleconnection index correlates with the summer FTLE anomalies confirming their role as a seasonal predictor for winter precipitation over the Iberian Peninsula.

1 Introduction

Seasonal forecast in mid-latitudes is still an open research field. However, the importance of this scale is relevant for different sectors such as agriculture (Howden et al., 2007; Meza et al., 2008), health (Thomson et al., 2008), energy (García-Morales and Dubus, 2007), or the financial sector (Meza et al., 2008). Most of Europe is located in the mid-latitude belt, where the changing nature of the atmosphere characteristics makes the seasonal climate forecast a difficult task. Thus, any tool to improve the forecast skill is potentially of great interest.

Two of the most important patterns that influence European climate variability are the North Atlantic Oscillation (NAO) and El Niño Southern Oscillation (ENSO) (Visbeck et al., 2003; Brönnimann, 2007). The indices of these large-scale climatic patterns are used as predictors for seasonal forecast over Europe. However, the relationship between NAO and ENSO and the European variability is nonstationary; that is, the strength of the correlation between these two teleconnections and climate anomalies has changed over time. These patterns, though dominant on a large scale, often fail to provide forecast skill in local regions. Precipitation predictability in Europe using NAO and ENSO as predictors is limited due to nonstationary (Vicente-Serrano and López-Moreno, 2008; Rodríguez-Fonseca et al., 2016). One way to advance the seasonal forecast would

be to identify new predictors in order to help improve the forecast. Previous works have shown a possible link between the Iberian precipitation and other variables like summer Sea Surface Temperature (SST) anomalies over the north Atlantic basin (Rodríguez-Fonseca and deCastro, 2002; Lorenzo et al., 2010; Hatzaki et al., 2015), other teleconnection patterns (deCastro et al., 2006; Casanueva et al., 2014) or the Euroasian snow cover in autumn (Brands et al., 2014). The storm track activity

5 has been related to the occurrence of extreme events (Lehmann and Coumou, 2015). Changes in mid-latitude circulation can strongly affect the weather events.

The atmosphere large-scale circulation causes mixing of air masses modifying the global moisture distribution, and therefore the rainfall patterns over the continents. One approach to characterize mixing and transport is by calculating Lagrangian trajectories of passive tracers in the atmosphere. Among the different statistics that can be calculated, finite-time Lyapunov

10 exponents (FTLE) measure the separation of two trajectories over time from initially nearby starting points, i.e. the local mixing rates at a finite time (Shadden et al., 2005). Among others, FTLE have been used to identify the presence of barriers to mixing in the atmosphere between the tropics and extratropics (Pierrehumbert and Yang, 1993), to study the zonal stratospheric jet (Beron-Vera et al., 2008), jet-streams (Tang et al., 2010), hurricanes (Rutherford et al., 2012), transient baroclinic eddies (von Hardenberg and Lunkeit, 2002), the spread of plankton blooms (Huhn et al., 2012), the polar vortex (Koh and Legras,

15 2002), or the atmospheric rivers (Garaboa-Paz et al., 2015).

Our goal in this study is to characterize the rainfall patterns in the Iberian Peninsula as a function of the large-scale tropospheric mixing over the Atlantic ocean. To that end, we have calculated a climatology of FTLE for the period $1979 - 2008$. The obtained time series was then correlated with the precipitation over the Iberian Peninsula. Finally, we discuss the obtained results by considering their relationship to the main modes of circulation variability.

2 Methods

2.1 Data

The atmospheric transport has been studied using wind field data retrieved from the European Center for Medium-Range Weather Forecast reanalysis, ERA-Interim (Dee et al., 2011), with a horizontal spatial resolution of $0.7°$, a vertical resolution of 100 hPa and a temporal resolution of 6 hours.

25 Gridded dataset for daily precipitation (mm) from 1979 to 2008 in Iberian Peninsula was used (IB02). This dataset corresponds to the continental area of both Iberian countries on a high resolution ($0.2°$) grid. It is the combination of two different datasets; PT02 (Belo-Pereira et al., 2011) and SPAIN02 (Herrera et al., 2012).

Yearly anomalies of the SST, geopotential at 500 hPa, sea level pressure (SLP) and wind at 200 hPa and 850 hPa for the same period have been used. The SST anomalies have been derived from *The Extended Reconstructed Sea Surface Tempera-*

30 *ture* (ERSST) dataset which is a global monthly sea surface temperature dataset derived from the International Comprehensive Ocean-Atmosphere Dataset (ICOADS). It has been derived on a $2° \times 2°$ grid with spatial completeness enhanced using statistical methods. This monthly analysis begins in January 1854 continuing nowadays. The newest version of ERSST, version 4, is based on optimally tuned parameters using the latest datasets and improved analysis methods. The geopotential, SLP and

wind anomalies have been obtained from the National Center of Environmental Prediction (NCEP) reanalysis with a spatial resolution of $2.5° \times 2.5°$. The climatology used for the anomaly plots is for the $1979 - 2008$ period.

The teleconnection indices NAO, SCA (Scandinavia pattern), EA (East Atlantic pattern), EA/WR (East Atlantic/ West Russia pattern), POL (The Polar/ Eurasia pattern), SOI (Southern Oscillation Index), PNA (Pacific-North American Pattern) and

5 the atmospheric mode AO (Artic Oscillation) were obtained from the Climate Prediction Center (CPC) at NCEP at monthly time scales. The monthly indices were averaged for the seasons JFM, AMJ, JAS and OND from 1979 to 2008. The most representative atmospheric patterns for the Northern Hemisphere were considered in order to analyze their influence on precipitation for the Iberian Peninsula and with the summer FTLEs.

The Pearson product-moment correlation coefficient t was considered to quantify the linear relationship between the anoma-

10 lies of the FTLE and precipitation, and the significance of this coefficient was assessed to be greater than 95% in terms of the Student's t-test.

2.2 Finite-Time Lyapunov Exponents (FTLE)

In a longitude-latitude-pressure coordinate system (ϕ, θ, P), the position of an air particle is calculated as,

$$
\begin{aligned}
\dot{\phi} &= \frac{u}{R\cos(\theta)} \\
\dot{\theta} &= \frac{v}{R} \\
\dot{P} &= w(\phi, \theta, P, t)
\end{aligned}
\tag{1}
$$

where, u, v and w are the eastward, northward and vertical wind components, respectively, and R is the Earth's mean radius. A fine grid of particles with an initial separation of $0.35°$ is uniformly distributed on the 850 hPa level covering the domain $(\theta, \phi) \in [0, 360] \times [-85, 85]$ at time instant t_0. Then, 3D Lagrangian simulations have been performed so that particle trajec-

20 tories are computed integrating Eq. (2) using a 4-th order Runge-Kutta scheme with a fixed time step of $\Delta t = 1.5$ hours, and multilinear interpolation in time and space.

In order to characterize the atmospheric transport, we introduce the finite-time Lyapunov exponents (FTLE), that measure, at a given location, the maximum stretching rate of an infinitesimal fluid parcel over the interval $[t_0, t_0 + \tau]$ starting at $\mathbf{r}(t_0) = \mathbf{r_0}$ and ending at $\mathbf{r}(t_0 + \tau)$ (Shadden et al., 2005; Sadlo and Peikert, 2007). The integration time τ must be predefined and it has

25 to be long enough to allow trajectories to explore the coherent structures present in the flow. The FTLE fields λ are computed along the trajectories of Lagrangian tracers in the flow as (Peacock and Dabiri, 2010),

$$
\lambda(\mathbf{r}_0, t_0, \tau) = \frac{1}{|\tau|} \log \sqrt{\mu_{max}(\tilde{\mathbf{C}}(\mathbf{r}_0))},
\tag{2}
$$

where μ_{max} is the maximum eigenvalue of the pull-back Cauchy-Green deformation tensor $\tilde{\mathbf{C}}$ over a sphere (Haller and Beron-Vera, 2012) which does not take into account the deformation due to vertical movement. Repelling (attracting) coherent

30 structures for $\tau > 0$ ($\tau < 0$) can be thought of as finite-time generalizations of the stable (unstable) manifolds of the system. These structures govern the stretching and folding mechanism that control flow mixing.

Nonlinear Processes
in Geophysics

Discussions

EGU

Ridges in the FTLE field are used to estimate finite time invariant manifolds in the flow that separate dynamically different regions, and organize air masses transport. A positive time direction (forward FTLE) integration leads to identify lines of maximal divergence of air masses. In contrast, a negative time direction integration, leads to identify areas of maximal convergence (backward FTLE).

5   A 30-years, $1979-2008$, time series of the FTLE field has been computed by following the same steps explained previously, but varying the initial time t_0 in fixed steps $\Delta t_0 = 6$ hours in order to release a new initial tracer grid. Each FTLE field obtained for each advection from $[t_0, t_0 + \tau]$ is an element of the time series $\lambda_i = \lambda(\mathbf{r_0}, t_0 + i\Delta t_0, \tau)$. FTLE anomalies were calculated from the FTLE median for the period $1979-2008$.

3   Results

10   We have studied the transport of air masses in terms of their FTLE from a climatological point of view. Figure 1(a) shows the FTLE for a given time at 850 hPa over the ocean. These structures reflect the large scale advection of air masses which are stretched and folded as wind transport them. The presence of ridges correspond to repelling manifolds where flow diverges. Time averaged FTLE maps for the $1979-2008$ period are shown in Figs. 1(b,c) for seasons January-March and July-September, respectively. As it was expected, in both cases, three latitudinal bands can be clearly identified in coincidence with the large

15   scale atmospheric circulation belts. For mid-latitudes, FTLE values are approximately two times higher than for the equatorial zone and large-scale mixing is generally higher in winter than in summer.

Westerly winds blowing across the Atlantic bring moist air into Europe. As the FTLE can be considered a measure of the large-scale tropospheric mixing (Garaboa-Paz et al., 2015), their role into winter rainfall in the Iberian Peninsula has been considered. Figure 2 shows the lead-lag correlation between winter (JFM) precipitation in Iberian Peninsula and the anomalies

20   of the FTLE from the North Atlantic East Ocean for three different seasons through the period $1979-2008$.

The values obtained for the spring (Fig. 2(a)) and autumn (Fig. 2(c)) are not significant. However, the correlations obtained for summer anomalies FTLE values (Fig. 2(b)) show large negative correlations, spatially consistent and statistically significant between the precipitation of the western half of the peninsula and the FTLE. In other words, for larger negative summer FTLE anomalies (low values of the large-scale tropospheric mixing) in the eastern Atlantic ocean, next winter precipitation over the

25   western Iberian Peninsula will also be larger. This result suggests the possibility of using the FTLE as a tool to forecast the occurrence of significantly rainy winters in the considered area with some months in advance.

The summer FTLE of the Eastern North Atlantic (ENA) area that show the higher correlation values with the winter precipitation cover approximately the area between $30°$W and $0°$W and between $25°$N and $65°$N. The size of the ENA was varied within the North Atlantic ocean without modifying significantly the results shown here.

30   To gain insight into the observed correlations, positive and negative FTLE anomaly maps have been discussed in terms of the atmospheric circulation and the atmosphere-ocean interactions. Spatial patterns of atmospheric circulation and SST anomalies were calculated for the period $1979-2008$. Previous studies have shown that SST anomalies in certain areas of the subtropical

North Atlantic are statistically related to winter precipitation on the IPNA region with a five-month lag (Rodríguez-Fonseca and deCastro, 2002).

Figure 3 shows the ratio between the positive (a) and negative (b) summer FTLE anomalies and the summer FTLE mean, respectively, and the summer SST anomalies calculated for the North Atlantic basin (c,d). Large values of the positive FTLE

5 anomalies (a) correspond to a larger activity of the storm track and its displacement to the south during summer, in agreement with a weakening of the Azores anticyclone and negative SST anomalies for the middle North Atlantic Ocean, Fig. 3(c). On the contrary, low values of the negative FTLE anomalies (b) are associated to highs blocking the pass of cold fronts, thus reducing the large-scale atmospheric mixing. This pattern coincides with large positive SST anomalies observed during summer for the mid North Atlantic Ocean, Fig. 3(d). Both figures for SST anomalies (c,d) have a resemblance with the so-called *summer North*

10 *Atlantic Horseshoe* (HS) SST pattern although displaced to the northwest. Previous works have found a relationship between summer SST anomalies for different areas of the North Atlantic basin and winter precipitation in Europe (Rodríguez-Fonseca and deCastro, 2002; Cassou et al., 2004). In our case, changes in the large-scale tropospheric mixing during summer, measured in terms of the FTLE anomalies and also observed in the summer SST anomalies, are related with the winter precipitation over Spain and Portugal. This result is in agreement with Lehmann and Coumou (2015) and Dong et al. (2013) that observe a strong

15 connection between changes in the mid-latitude circulation and weather events.

In addition, Anomaly maps for the geopotential at 500 hPa, Fig. 4, show that positive summer FTLE anomalies correspond to the next winter positive height anomalies occurring over western coast of Europe (a). On the contrary, summer FTLE negative anomalies correspond to next winter trough, that it is a region with relatively lower heights, occurring over the western coast of Europe and in particular over the western Iberian Peninsula (b). These troughs are associated to cloudy conditions and precipitation. A

20 similar pattern is observed for the SLP anomaly patterns (not shown here).

In addition, winter wind anomalies for 200 hPa and 850 hPa are shown in Fig. 5. For the anomalies at 200 hPa associated with positive FTLE (a), latitudes between $40°$N and $50°$N show less wind than normal. This can be related to a weaker than normal jet stream. As the jet stream defines the storm track, a weaker jet stream means that lows traveling the Atlantic do not reach the Iberian Peninsula with the expected frequency. Moreover, taking into account that winds are larger at latitudes

25 $≈ 30°$N (Fig. 5(a)) and that geopotential anomalies show high pressures over the NE Atlantic and low pressures located at NW Atlantic (Fig. 4(a)) we can hypothesize that the meridional variability of the jet stream increases under these circumstances. Figure 5(c) shows less wind at 850 hPa in the trajectory between Caribbean area and the Iberian Peninsula related to a less frequent arrival of cold fronts and their associated baroclinic structures. Figures 5(b,d) show the inverse situation. In Fig. 5(b) there are no significant anomalies in the storm track. Therefore, jet stream is in its normal location and the Iberian Peninsula

30 is affected by low pressure systems at its normal frequency. However, note in Fig. 5(d) that for low latitudes the connection between the Caribbean area and the Iberian Peninsula is reinforced, meaning that rainfall may be stronger, associated with the enhancement of the poleward transport of moisture.

Finally, summer anomalies of the FTLE and winter precipitation in the Iberian Peninsula have been correlated to different teleconnection patterns. Table 1 summarizes the main results. Note that summer anomalies of the FTLE correlate with a

35 significance greater than 95% with summer and autumn EA index, which also correlates with winter rainfall. EA index is the

Table 1. Seasonal correlations between summer FTLE anomalies, winter rainfall and different teleconnection indices; the North Atlantic Oscillation (NAO), the East Atlantic Pattern (EA), the East Atlantic/Western Russia (EA/WR), the Scandinavian Pattern (SCA), the Pacific/North American teleconnection pattern (PNA), the Southern Oscillation Index (SOI), and the Arctic Oscillation (AO). Only significan values are shown. (*) and (**) stand for significances larger than 95% and 90%, respectively.

Summer FTLE							
Season/index	NAO	EA	EA/WR	SCA	PNA	SOI	AO
jfm						-0,24*	
amj	0,34**				0,23*		
jas		0,46**		-0,26*	0,32**		0,25*
ond		-0,54**		-0,27*	-0,30**		0,29*
Winter Rainfall							
Season/index	NAO	EA	EA/WR	SCA	PNA	SOI	AO
jfm	-0,58**		-0,32**	0,69**		0,37**	-0,52**
amj				0,27*			
jas		-0,38**			-0,25*		
ond		0,46**		0,36**			-0,48**

second mode of inter-annual variability of the tropospheric circulation of the North Atlantic. Previous work have found that in southern Europe the EA pattern is at least as important as the NAO for explaining inter-annual variations of sensible climate variables such as air temperatures, sea-surface temperatures, precipitation or wind (Serrano et al., 1999; Saenz et al., 2001; Comas-Bru and McDermott, 2013; Casanueva et al., 2014). Besides, some recent studies suggest that the EA pattern may play a role in positioning the primary North Atlantic storm track (Seierstad et al., 2007; Woollings et al., 2010). Note as well in Table 1 that the autumn SCA pattern also correlates with the summer FTLE anomalies although less significant than EA (90% significant), and this pattern influence the winter precipitation. The Scandinavian pattern (SCA) is the third leading mode of winter SLP variability in the European region equivalent to the Eurasia-1 pattern described by Barnston and Livezey (1987) and other studies also show its influence on the Iberian Peninsula precipitation (deCastro et al., 2006; Casanueva et al., 2014).

4   Conclusions

In the present study, the connection between winter precipitation over the Iberian Peninsula and the finite-time Lyapunov exponents (FTLE) calculated over the eastern Atlantic ocean has been investigated. A significant negative correlation was observed between the summer FTLE anomalies and winter precipitation over the western Iberian Peninsula. The conclusions suggest the possibility of predicting the occurrence of rainy winters using these exponents several months in advance.

Summer anomalies of the FTLE have also been correlated to other circulation and temperature patterns as SST, SLP or the geopotential. In all cases, negative summer FTLE anomalies correspond to well known patterns of precipitation over western

Iberian Peninsula. Low values of tropospheric mixing (negative FTLE anomalies) during summer correspond to positive SST anomalies and highs blocking the passage of fronts over the western Europe. However, wind, SLP and geopotential anomalies during next winter show the opposite relationship as lows may reach the Iberian Peninsula, in agreement with the negative correlation observed between summer FTLE and winter precipitation. Finally, the relationship with some teleconnection pat-

5   terns of the Northern Hemisphere was shown in Table 1. Once more, summer FTLE anomalies correlate with summer and next autumn EA indices which influence on winter rainfall patterns of the Iberian Peninsula.

References

Barnston, A.G. and Livezey, R.E. Classification, seasonality and persistence of low-frequency atmospheric circulation patterns. *Monthly Weather Review 115*, 1083–1126, 1987.

Belo-Pereira, M., Dutra, E., and Viterbo , P. Evaluation of global precipitation datasets over the Iberian Peninsula, *J. Geophys. Res. 116*, D20101, 2011.

Beron-Vera, F.J., M.G. Brown, Olascoaga, M.J., I.I. Rypina, H. Kocak, and I.A. Udovydchenkov, Zonal jets as transport barriers in planetary atmospheres, *J. Atmos. Sci. 65*, 3316–3326, 2008.

Brands, S., Herrera, S., and Gutiérrez, J.M. Is Eurasian snow cover in October a reliable statistical predictor for the wintertime climate on the Iberian Peninsula? *International Journal of Climatology 345*, 1615–1627, 2014.

Brönnimann, S. The impact of El Niño/Southern Oscillation on European climate, *Review of Geophysics 45*, RG3003, 2007.

Casanueva, A., Rodríguez-Puebla, C., Frías, M.D., and González-Reviriego, N. Variability of extreme precipitation over Europe and its relationships with teleconnection patterns. *Hydrology and Earth System Sciences 18*, 709–725, 2014.

Cassou, C., Deser, C., Terray, L., Hurrell, J.W., and Drevillon, M. Summer Sea Surface Temperature Conditions in the North Atlantic and Their Impact upon the Atmospheric Circulation in Early Winter. *Journal of Climate 17*, 3349–3363, 2004.

Comas-Bru, L. and McDermott, F. Impacts of the EA and SCA patterns on the European twentieth century NAO-winter-climate relationships. *Q. J. R. Meteorol. Soc. 140*, 354–679, 2013.

deCastro, M., Lorenzo, M.N., Taboada, J.J., Sarmiento, M., Alvarez, I., Gómez-Gesteira, M. Influence of teleconnection patterns on precipitation variability and on river flow regimes in the Miño River basin (NW Iberian Peninsula). *Clim. Res. 32*, 63–73, 2006.

Dee, D.P., S. M. Uppala, A.J. Simmons, P. Berrisford, P. Poli, S. Kobayashi, U. Andrae, M. A. Balmaseda, G. Balsamo, P. Bauer, P. Bechtold, A. C. M. Beljaars, L. van de Berg, J. Bidlot, N. Bormann, C. Delsol, R. Dragani, M. Fuentes, A.J. Geer, L. Haimberger, S. B. Healy, H. Hersbach, E. V. Holm, L. Isaksen, P. Kallberg, M. Koehler, M. Matricardi, A. P. McNally, B. M. Monge-Sanz, J.J. Morcrette, B.K. Park, C. Peubey, P. de Rosnay, C. Tavolato, J.N. Thepaut, and F. Vitart. The ERA-Interim reanalysis: configuration and performance of the data assimilation system, *Q. J. Roy. Meteo. Soc. 137*, 553–597, 2011.

Dong, B., Sutton, R., Woolings, T., and Hodges, K. Variability of the North Atlantic summer storm track: mechanisms and impacts on European climate. *Environ. Res. Lett. 8*, 034037, 2013.

Garaboa-Paz, D., Eiras-Barca, J., Huhn, F., and Pérez-Muñuzuri, V. Lagrangian coherent structures along atmospheric rivers. *Chaos 25*, 063105, 2015.

García-Morales, M. and Dubus, L. Forecasting precipitation for hydroelectric power management: how to exploit GCM's seasonal ensemble forecasts, *International Journal of Climatology 27*, 1691–1705, 2007.

Haller, G., and Beron-Vera F.J. Geodesic theory of transport barriers in two-dimensional flows. *Physica D 241*, 1680–1702, 2012.

Hatzaki, M. and Renguang, W. The south-eastern Europe winter precipitation variability in relation to the North Atlantic SST. *Atmospheric Research 152*, 61–68, 2015.

Herrera, S., Gutiérrez, J.M., Ancell, R., Pons, M.R., Fías, M.D., and Fernández, J. Development and analysis of a 50-year high-resolution daily gridded precipitation dataset over Spain (Spain02), *Int. J. Climatol. 32*, 74–85, 2012.

Howden, S.M. Soussana, J.F., Tubiello, F.N., Chhetri, N., Dunlop, M., and Meinke, H. Adapting agriculture to climate change, *Proceedings of the National Academy of Science 104*, 19691–19696, 2007.

Huhn, F., von Kameke, A., Allen-Perkins, S., Montero, P., Venancio, A., and Pérez-Muñuzuri, V.: Horizontal Lagrangian transport in a tidal driven estuary: Transport barriers attached to prominent coastal boundaries, *Continental Shelf Res. 30–40*, 1–13, 2012.

Koh, T.Y., and Legras, B. Hyperbolic lines and the stratospheric polar vortex, *Chaos 12*, 382–394, 2002.

Lehmann, J. and Coumou, D. The influence of mid-latitude storm tracks on hot, cold, dry and wet extremes. *Sci. Rep. 5*, 17491, 2015.

5 Lorenzo, M.N., Iglesias, I., Taboada, J.J., and Gómez-Gesteira, M. Relationship between monthly rainfall in northwest Iberian Peninsula and North Atlantic sea surface temperature. *International Journal of Climatology 30*, 980–990, 2010.

Meza, F.J., Hansen, J.W., and Osgood, D. Economic Value of Seasonal Climate Forecasts for Agriculture: Review of Ex-Ante Assessments and Recommendations for Future Research, *Journal of Applied Meteorology and Climatology 47*, 1269–1286, 2008.

Peacock, T. and Dabiri, J.O. Introduction to Focus Issue: Lagrangian Coherent Structures, *Chaos 20*, 017501, 2010.

10 Pierrehumbert, R.T., and H. Yang. Global chaotic mixing on isentropic surfaces, *J. Atmos. Sci. 50*(15), 2462–2480, 1993.

Rodríguez-Fonseca, B. and deCastro, M. On the connection between winter anomalous precipitation in the Iberian Peninsula and North West Africa and the summer subtropical Atlantic sea surface temperature *Geophysical Research Letters 29*, 1863, 2002.

Rodríguez-Fonseca, B., Suárez-Moreno, R., Ayarzagüena, B., López-Parages, J., Gómara, I., Villamayor, J., Mohino, E., Losada, T., and Castaño-Tierno, A. A Review of ENSO Influence on the North Atlantic. A Non-Stationary Signal. *Atmosphere 7*, 87, 2016.

15 Rutherford, B., G. Dangelmayr, and M.T. Montgomery, Lagrangian coherent structures in tropical cyclone intensification, *Atmos. Chem. Phys. 12*(12), 5483–5507, 2012.

Sadlo, F., and Peikert, R. Efficient visualization of Lagrangian coherent structures by filtered AMR ridge extraction, *IEEE Transactions on Visualization and Computer Graphics 13*, 1456–1463, 2007.

Saenz, J., Rodríguez-Puebla, C., Fernández, J., and Zubillaga, J. Interpretation of interannual winter temperature variations over southwestern
20 Europe. *J. Geophys. Res. 106*, 20641–20651, 2001.

Seierstad, I.A., Stephenson, D.B., and Kvamsto, N.G. How useful are teleconnection patterns for explaining variability in extratropical storminess? *Tellus Ser. A 59*, 170–181, 2007.

Serrano, A., García, J.A., Mateos, V.L., Cancillo, M.L., and Garrido, J. Monthly Modes of Variation of Precipitation over the Iberian Peninsula. *J. Climate 12*, 2894–2919, 1999.

25 Shadden, S.C., Lekien, F., and Marsden, J. Definition and properties of Lagrangian coherent structures from finite-time Lyapunov exponents in two-dimensional aperiodic flows, *Physica D 212*, 271–304, 2005.

Tang, W., M. Mathur, G. Haller, D.C. Hahn, and F.H. Ruggiero, Lagrangian Coherent Structures near a Subtropical Jet Stream, *J. Atmos. Sci. 67*(7), 2307–2319, 2010.

Thomson, M.C., García-Herrera, R., and Beniston, M. eds. Seasonal Forecasts, Climatic Change and Human Health. New York: Springer.
30 234 pp, 2008.

Vicente-Serrano, S.M., and López-Moreno, J.I. Nonstationary influence of the North Atlantic Oscillation on European precipitation, *J. Geophys. Res. 113*, D20120, 2008.

Visbeck, M., Chassignet, E., Curry, R., Delworth, T., Dickson, B., and Krahmann, G. The Ocean's Response to North Atlantic Oscillation Variability. In: The North Atlantic Oscillation: Climate Significance and Environmental Impact, Hurrell, J.W., Y. Kushnir, G. Ottersen and
35 M. Visbeck (eds) American Geophysical Union: Washington, DC; 113–146, 2003.

von Hardenberg, J., and A.F. Lunkeit, Transient chaotic mixing during a baroclinic life cycle, *Chaos 10*(1), 1054–1500, 2000.

Woollings, T., Hannachi, A., and Hoskins, B. Variability of the North Atlantic eddy-driven jet stream. *Q. J. R. Meteorol. Soc. 136*, 856–868, 2010.
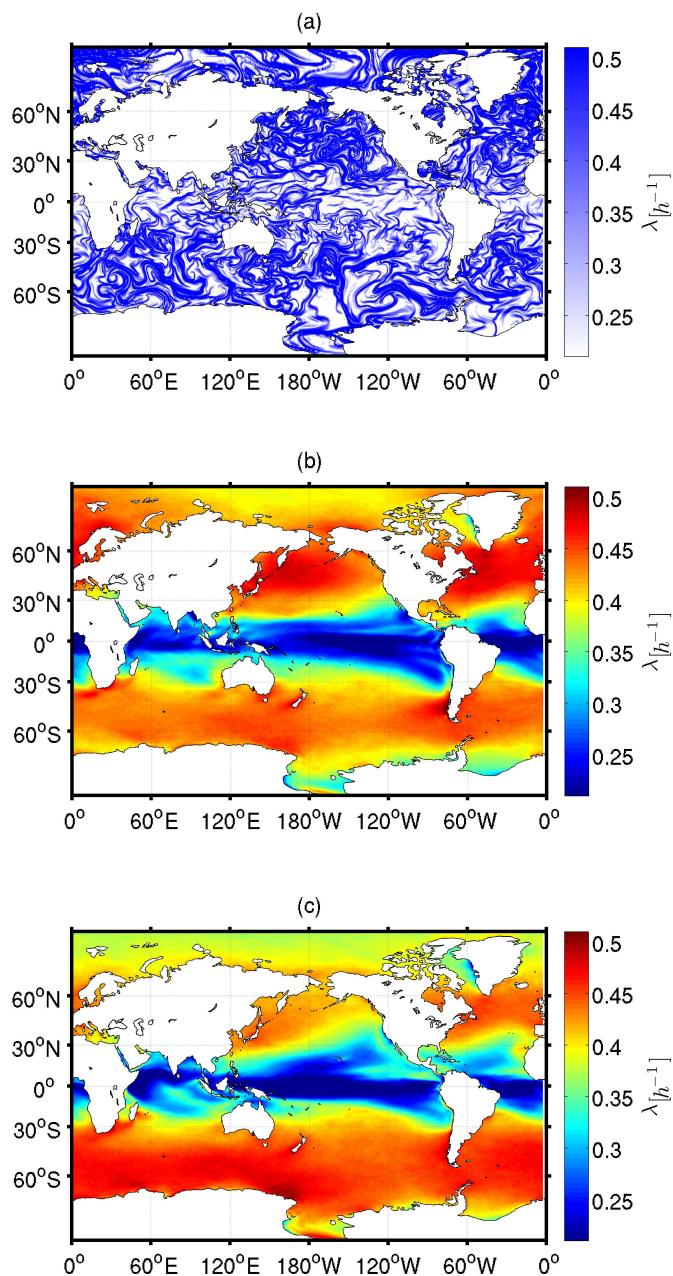
Figure 1. Finite-time Lyapunov exponents λ (a). Local maxima in the plot (darker colors) are potential repelling Lagrangian coherent structures. Mean FTLE climatology for periods January-March (b) and July-September (c) for the $1979 - 2008$ time series. $\tau = 5$ days.
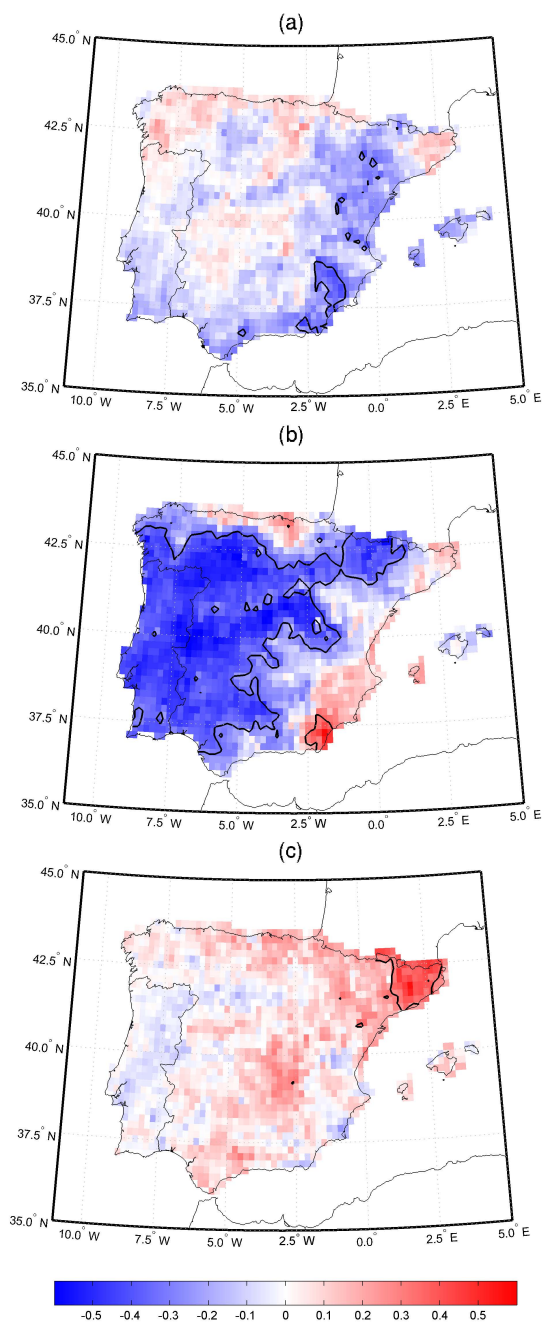
Figure 2. Correlation map between winter precipitation of the Iberian Peninsula and the FTLE anomalies for the Eastern Atlantic region ($[30°W, 0°W] \times [25°N, 65°N]$) for the three previous seasons; a) spring (AMJ), b) summer (JAS) and c) autumn (OND). The black lines mark the significant correlation at 95%.
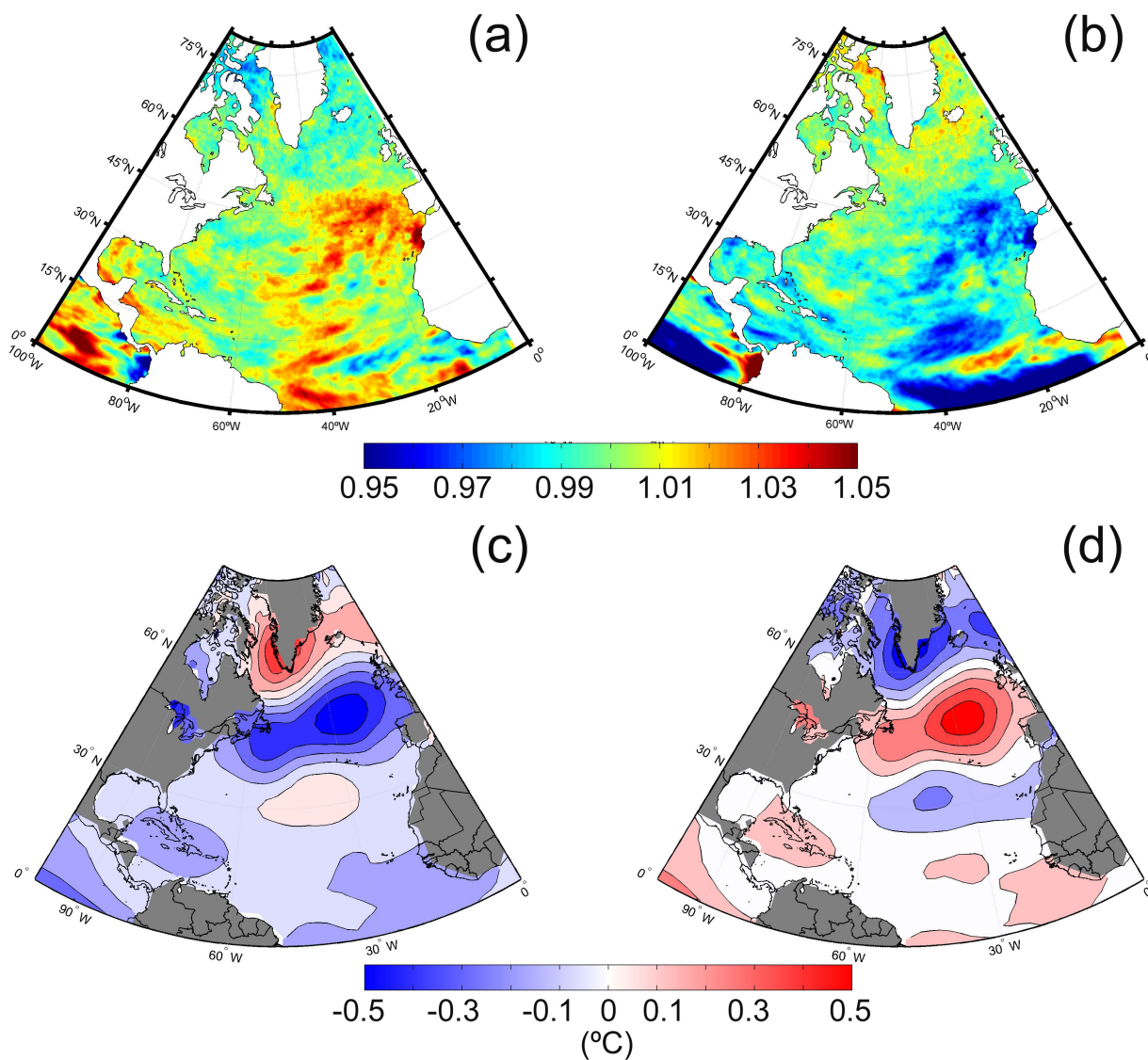
Nonlinear Processes
in Geophysics

Discussions

Open Access

EGU

Figure 3. Ratio between the positive (a) and negative (b) summer FTLE anomalies and the global summer FTLE mean. Summer SST anomalies in the Atlantic ocean for years with positive (c) and negative (d) summer FTLE anomalies, respectively.
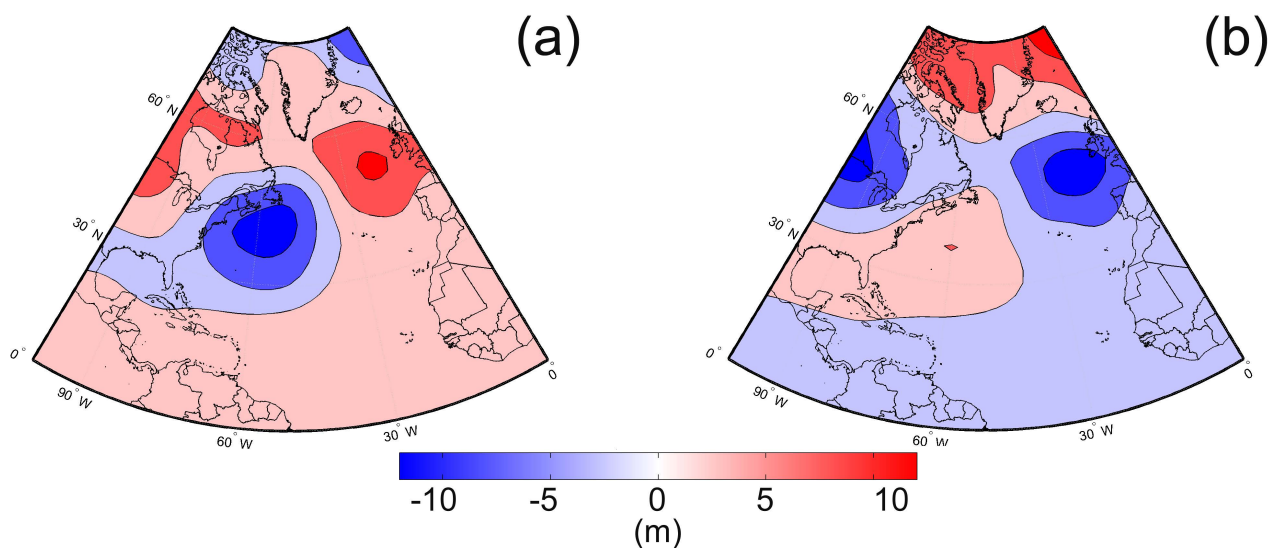
Nonlinear Processes
in Geophysics
Discussions

Open Access

EGU

Figure 4. Geopotential at 500 hPa anomalies in the Atlantic for winter. (a) and (b) correspond to years with positive and negative summer FTLE anomalies, respectively.
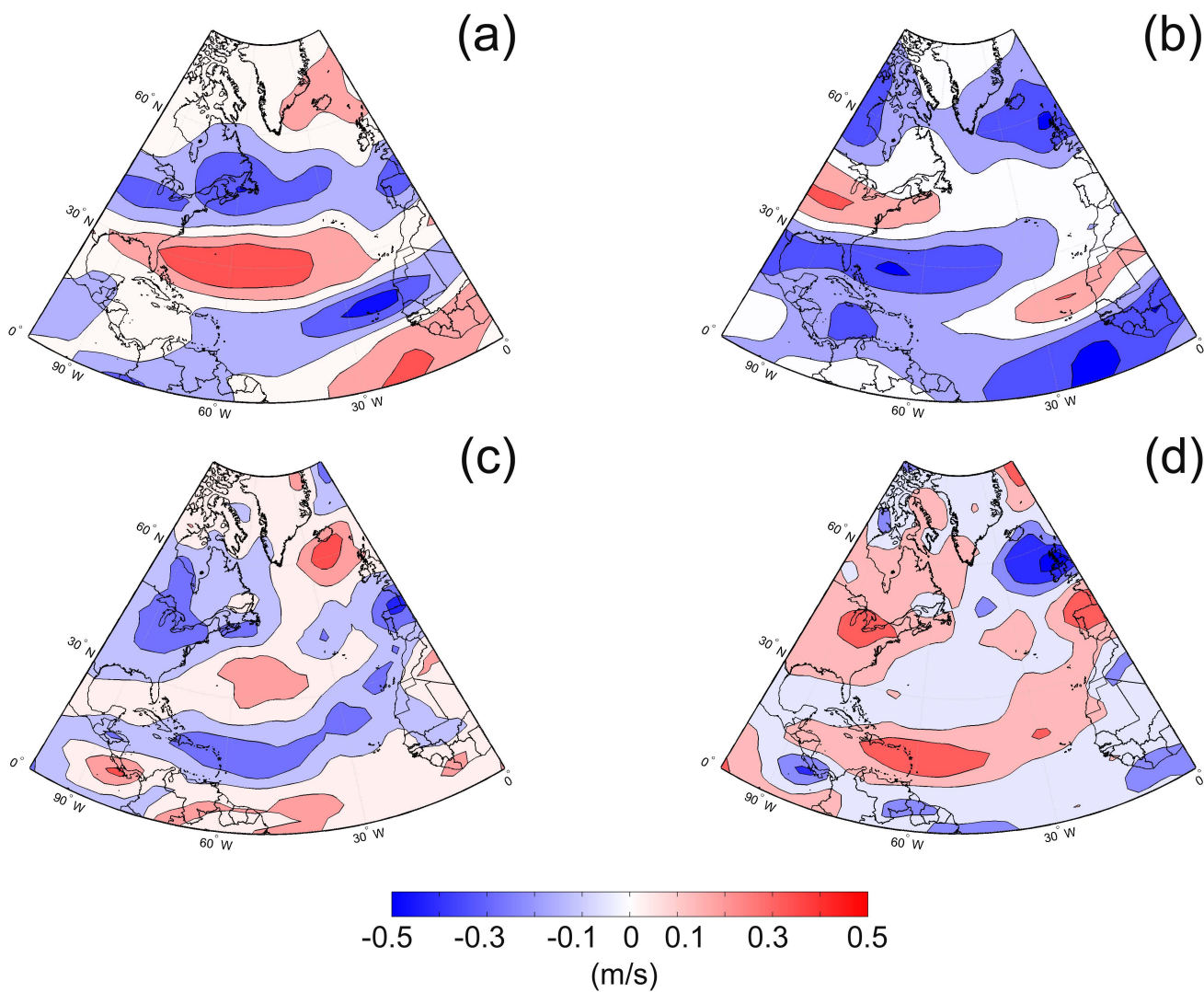
Figure 5. Wind anomalies in the Atlantic for winter. (a/b) and (c/d) correspond to years with positive/negative summer FTLE anomalies for 200 hPa and 850 hPa, respectively.